Volume 16
Number 21
7 June 2025
Pages 9033–9544

Chemical Science

rsc.li/chemical-science

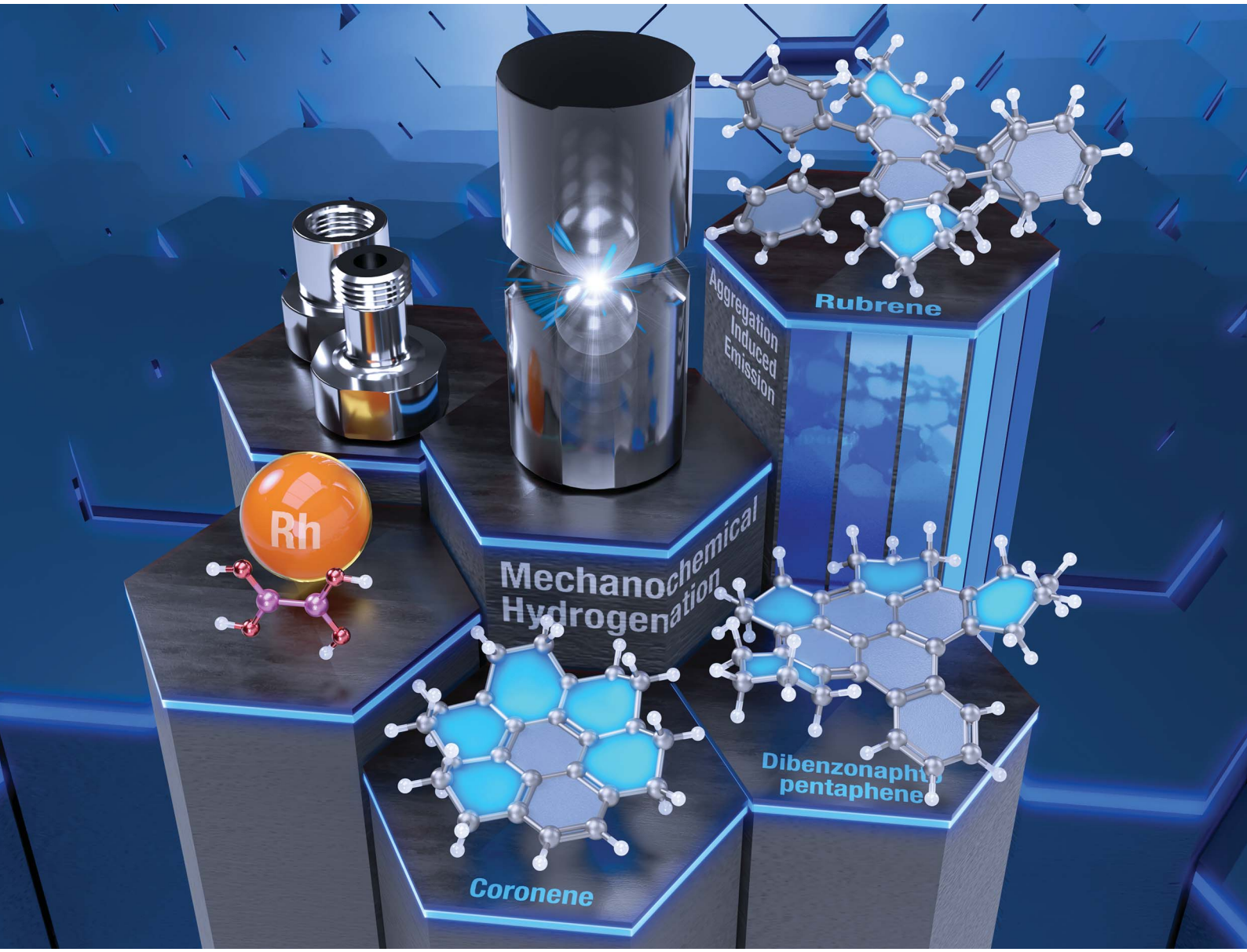

ISSN 2041-6539

ROYAL SOCIETY OF CHEMISTRY

EDGE ARTICLE

Kenichiro Itami, Hideto Ito *et al.*

Rh-catalyzed mechanochemical transfer hydrogenation for the synthesis of periphery-hydrogenated polycyclic aromatic compounds

15 YEARS ANNIVERSARY

Chemical Science

ROYAL SOCIETY OF CHEMISTRY

EDGE ARTICLE

View Article Online
View Journal | View Issue

Cite this: *Chem. Sci.*, 2025, **16**, 9117

All publication charges for this article have been paid for by the Royal Society of Chemistry

Received 25th February 2025
Accepted 11th April 2025

DOI: 10.1039/d5sc01489a

rsc.li/chemical-science

Rh-catalyzed mechanochemical transfer hydrogenation for the synthesis of periphery-hydrogenated polycyclic aromatic compounds†

Yoshifumi Toyama, [a] Takumu Nakamura,[b] Yushin Horikawa,[a] Yuta Morinaka,[b] Yohei Ono,[b] Akiko Yagi, [ac] Kenichiro Itami *[cd] and Hideto Ito *[a]

Hydrogenated nanographene has attracted attention as a new class of nanocarbon material owing to its potential applications in various research fields. However, the synthesis of periphery-hydrogenated nanographenes or polycyclic aromatic hydrocarbons (PAHs) is a significant challenge because of the harsh conditions and poor solubility of the starting materials. Conventional solution-state conditions require high-pressure hydrogen gas and lengthy reaction times. In this study, we developed a novel approach utilizing rhodium-catalyzed mechanochemical transfer hydrogenation, which enables hydrogenation without using hydrogen gas. Various hydrogenated PAHs were rapidly obtained using a simple protocol under ambient atmosphere and air, with one PAH showcasing intriguing properties such as aggregation-induced emission. Thus, the demonstrated mechanochemical hydrogenation method is expected to contribute to the rapid and efficient synthesis of a novel class of sp^2/sp^3-carbon-conjugated hydrocarbons.

Introduction

Nanographene and polycyclic aromatic hydrocarbons (PAHs) are regarded as promising materials owing to their unique electronic, optical, and magnetic properties.[1] These materials are also attractive for applications in fields such as materials science and organic electronics, mainly because of their extended conjugated carbon structures, which allow for fine-tuning of their properties through molecular design. Recently, a notable increase in interest has been observed surrounding a novel class of nanocarbon material, namely, hydrogenated nanographenes/PAHs.[2–4] Some of these molecules, such as hydrogenated anthracene, corannulene, and coronene, have been proposed to exist as interstellar materials.[5] Of particular interest are periphery-hydrogenated PAHs, which possess high solubility and enhanced emission properties compared to those of mother PAHs. Moreover, these PAHs are anticipated to exhibit augmented electron–phonon interactions and universal characteristics such as a negative electron affinity associated with rigid sp^3-carbon-based nanocarbon materials.[3,4] Despite their prospective utilities, the accessibility of periphery-hydrogenated PAHs has been considerably constrained, primarily due to the difficulty of their synthesis.

The synthesis of periphery-hydrogenated PAHs has been achieved by employing transition metal catalysts such as Pd, Pt, Ni, Co, and Rh under high-pressure hydrogen gas atmospheres.[6] In the 1970s, hydrogenated PAHs such as hydrogenated pyrene, perylene, and benzo[*a*]anthracene were synthesized as a mixture of isomers under harsh conditions with high-pressure hydrogen gas at high temperature for many hours (Fig. 1A).[7–9] In 2004 and 2019, Müllen and Narita reported the synthesis of peralkylated coronene from hexabenzo[*bc*,*ef*,*hi*,*kl*,*no*,*qr*]coronene and peralkylated circumbiphenyl from ovalene using Pd/C and H_2 (65–150 bar) at 65–120 °C (Fig. 1B).[3,4] As demonstrated previously, the hydrogenation of larger PAHs still necessitates harsh conditions. The presence of bulky moieties, such as adamantane, of the aromatic core requires harsh conditions for hydrogenation albeit small PAH structures.[10] Another difficulty in the hydrogenation of PAHs is that PAHs are typically poorly soluble in conventional organic solvents due to strong intermolecular π–π and C–H/π interactions.[11] As a result, only few studies have been reported on the hydrogenation of PAHs, and the optimal hydrogenation techniques have still been under development.[12]

Recently, catalytic transfer hydrogenation methods for simple arenes without the use of H_2 gas were reported by

[a]*Graduate School of Science, Nagoya University, Chikusa, Nagoya 464-8602, Japan*
[b]*Tokyo Research Center, Advanced Materials Research Laboratory, Advanced Integration Research Center, Research Division, Tosoh Corporation, 2743-1 Hayakawa, Ayase, Kanagawa 252-1123, Japan*
[c]*Institute of Transformative Bio-Molecules (WPI-ITbM), Nagoya University, Chikusa, Nagoya 464-8602, Japan*
[d]*Molecule Creation Laboratory, Cluster for Pioneering Research, RIKEN, Wako, Saitama 351-0198, Japan*

† Electronic supplementary information (ESI) available: Syntheses, NMR, UV-vis absorption, emission, DFT calculations, and crystallographic table. CCDC 2389851, 2389852 and 2425787. For ESI and crystallographic data in CIF or other electronic format see DOI: https://doi.org/10.1039/d5sc01489a

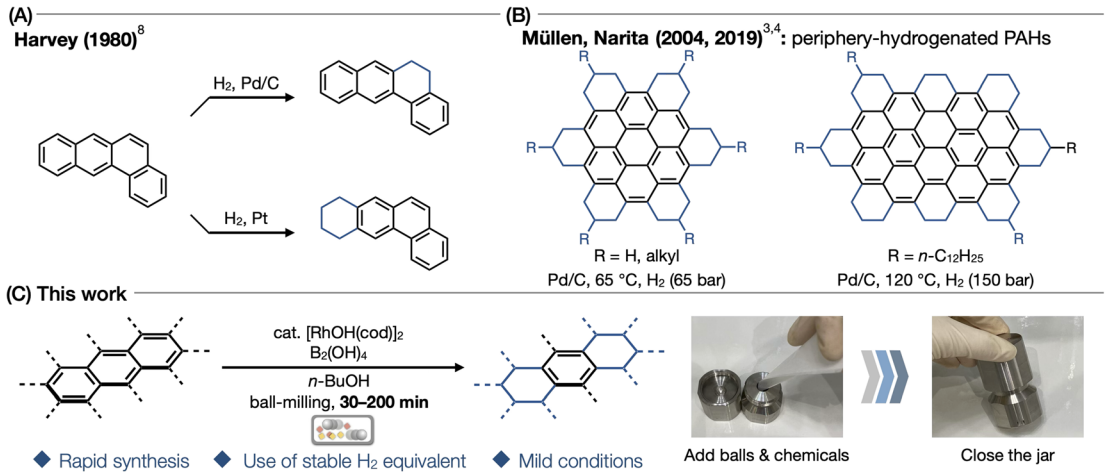

Fig. 1 (A) Hydrogenation of PAHs with transition metal catalysts. (B) Previous reports of periphery-hydrogenated nanographenes. (C) This work.

Glorius[13] and Dou,[14] (Fig. 1B). A key common feature of both reactions is the use of alcohol with ammonia borane (NH_3BH_3) or tetrahydroxydiboron $B_2(OH)_4$/EtOH as a source of hydrogen. During our recent research on the synthesis and transformation of nanocarbons by solution-state and/or mechanochemical methods,[15–17] we envisaged that this hydrogen-gas-free hydrogenation system would be beneficial for the mechanochemical hydrogenation of poorly soluble PAHs. Another benefit is that the general characteristics of mechanochemical reactions, such as the use of minimal or no solvent and rapid reaction under mild reaction conditions, are appropriate for achieving this challenging hydrogenation. Sajiki also demonstrated the utility of mechanochemical (planetary ball-milling) hydrogenation of simple arenes;[18] however, its applicability to larger PAHs has not been demonstrated. Furthermore, while related hydrogenations of ketone, alkene, alkyne, and nitro compound have been reported,[19–23] to the best of our knowledge, no study has been conducted on the mechanochemical catalytic transfer hydrogenation of PAHs.

Herein, we present the mechanochemical transfer hydrogenation of various PAHs in the presence of a Rh catalyst with diboronic acid and alcohol as a hydrogen source (Fig. 1C). Direct mixing of the Rh catalyst, diboronic acid, arenes, and *n*-butanol using a ball-milling machine in air enabled the hydrogenation of arenes within short duration. Depending on the reaction conditions and substrates, diverse unprecedented hydrogenation reactions occur to afford per- and/or periphery-hydrogenated PAHs.

Results and discussion

First, we optimized the reaction conditions for mechanochemical arene hydrogenation using phenylcyclohexane (**1**) (0.20 mmol, 1.0 equiv.) as a model substrate (Table 1). Following a previous study on catalytic transfer hydrogenation by Dou with slight modifications,[14] $B_2(OH)_4$ (8.0 equiv.) and *n*-BuOH (0.20 mL, 11 equiv.) was selected as an additive for the hydrogen source, with 5 mol% $[RhOH(cod)]_2$ (cod = 1,5-cyclooctadiene) as the catalyst (Table 1). In the optimal reactions, all reagents without *n*-BuOH, a stainless-steel ball (diameter of 7 mm), and *n*-BuOH were added in the given order to a 1.5 mL stainless-steel jar in air. The jar was then closed and placed in a mixer mill (Retsch MM400). After 60 min of ball milling at 30 Hz with direct heating using a heat-gun[15,24] (heat-gun preset temperature: 100 °C), the jar was opened, and the content was diluted with $CHCl_3$ and passed through a short pad of silica gel to remove the catalyst. ^{1}H NMR analysis and isolation resulted in the full conversion of **1** and the almost stoichiometric formation of cyclohexylcyclohexane (**2**) (99% NMR yield and 93% isolated yield). In contrast, the use of NH_3BH_3, $[RhCl(cod)]_2$, and 2,2,2-trifluoroethanol, whose conditions were proven to be effective by Glorius for the in-solution hydrogenation of benzene, naphthalene, pyridine, and indole derivatives,[13] dramatically diminished the yield of the desired product **2** (entry 2, 8%). Although the reaction was not complete within 1 min (entry 3, 21%), completion was observed even after 10 min reaction (entry 4, 99%). The reaction was then conducted at room temperature (20–25 °C) to afford **2** in 57% yield in 60 min along with the recovery of unreacted **1** (entry 5). Subsequently, various Rh sources such as $[RhCl(cod)_2]$, $Rh(BF_4)(cod)_2$, and RhCl(CAAC)(cod)[25] were examined instead of using $[RhOH(cod)]_2$ (entries 6–8), and the yield of each product did not exceed the yield of the reaction with $[RhOH(cod)_2]$. Unexpectedly, RhCl(CAAC)(cod),[25] which is known as an effective hydrogenation catalyst in the solution-state reaction, did not display any catalytic activity in the present mechanochemical system. When using ethanol with heating at 100 °C, the yield of **2** was reduced to 71% (entry 9). The volatile ethanol vapor was observed to leak from the reaction jar owing to heat-gun heating; thus, liquid-assisted grinding[26] did not work sufficiently. Other alcohol additives, i-PrOH and 2,2,2-trifluoroethanol, were also ineffective (entries 10 and 11). Interestingly, the reaction proceeded even when using solid alcohol reagents, D-(+)-glucose and β-cyclodextrin to afford **2** in 29% and 24% NMR yields, respectively (entries 12 and 13). As a result, the use of *n*-BuOH—a liquid primary alcohol with a high-boiling

Table 1 Screening of conditions for the mechanochemical hydrogenation of cyclohexylbenzene[a]

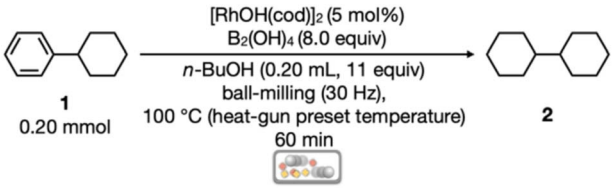

Entry	Deviation from the standard conditions	Yield of 2[b]
1	None	99% (93%)[c]
2	NH_3BH_3(1.5 equiv.), $[RhCl(cod)]_2$ (10 mol%), and 2,2,2-trifluoroethanol (0.20 mL) were used instead of $B_2(OH)_4$, $[RhOH(cod)]_2$, and *n*-BuOH	8%
3	Ball-milling for 1 min	21%
4	Ball-milling for 10 min	99%
5	Without heating (room temperature, 20–25 °C)	57%
6	$[RhCl(cod)]_2$ instead of $[RhOH(cod)]_2$	57%
7	10 mol% of $Rh(BF_4)(cod)_2$ instead of $[RhOH(cod)]_2$	14%
8	10 mol% of RhCl(CAAC)(cod)[24] instead of $[RhOH(cod)]_2$	9.5%
9	EtOH instead of *n*-BuOH	71%
10	i-PrOH instead of *n*-BuOH	35%
11	2,2,2-Trifluoroethanol instead of *n*-BuOH	Trace
12	D-(+)-Glucose (2.2 equiv.) instead of *n*-BuOH	29%
13	β-Cyclodextrin (0.5 equiv.) instead of *n*-BuOH	24%

[a] Reactions were conducted in a 1.5 mL stainless-steel jar using a stainless-steel ball with a diameter of 7 mm. [b] ^{1}H NMR yield using dibromomethane as an internal standard. [c] Isolated yield. Heat-gun preset temperature (100 °C) was indicated as the reaction temperature.

point (approximately 118 °C)—was considered optimal for the present mechanochemical hydrogenation reaction.

We then conducted the mechanochemical hydrogenation of naphthalene (**3**) to compare its activity with that of conventional solution-state hydrogenation. The reaction under Dou's conditions[14] using $B_2(OH)_4$/EtOH for solution-state transfer hydrogenation at 50 °C for 30 min resulted in the production of tetralin (**4a**) in 45% NMR yield (Fig. 2A). In this reaction, naphthalene was recovered in 45% NMR yield. Next, a room-temperature mechanochemical reaction with a reduced amount of EtOH for 10 min resulted in a similar result in terms of yield, although the reaction seemed to be faster than the solution-state reaction. However, a distinct difference was observed when the reaction time was extended to 30 min for mechanochemical hydrogenation; the fully hydrogenated product *cis*-decalin (**4b**) was isolated in 65% yield, whereas *trans*-decalin (**4c**) was not formed. These control experiments suggest that mechanochemical hydrogenation has advantages over conventional solution-based reactions in terms of the catalytic activity, reaction time, and temperature. In Dou's solution-state hydrogenation using $[RhOH(cod)]_2/B_2(OH)_4$/EtOH, the formation of heterogeneous Rh nanoparticles is

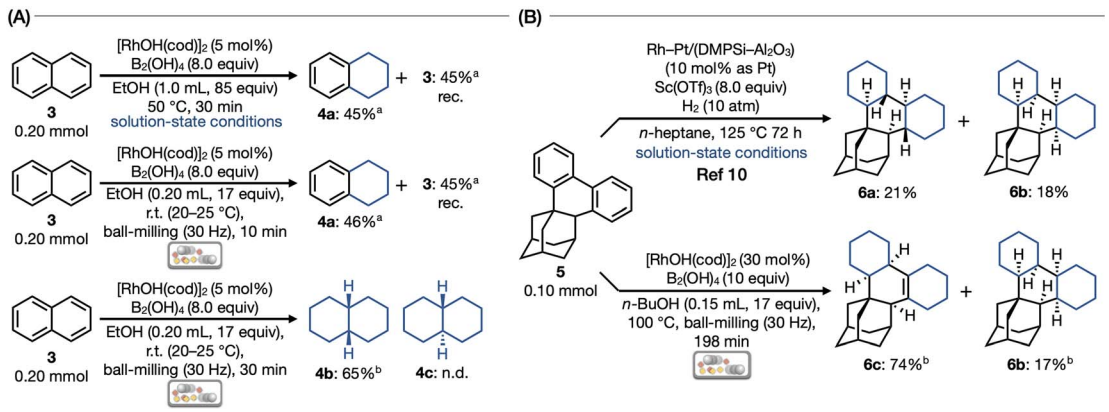

Fig. 2 Comparison of mechanochemical and solution-state conditions in the hydrogenation of (A) naphthalene and (B) adamantane-annulated biphenyl. Ball milling reactions were conducted in a 1.5 mL stainless-steel jar using a stainless-steel ball (diameter of 7 mm). [a] ^{1}H NMR yield using dibromomethane as an internal standard. [b] Isolated yield.

expected to be one of the active species.[14] In our mechanochemical reaction, we also expected that the similar heterogeneous Rh nanoparticle-catalyzed hydrogenations occur because of preferential formation of *cis*-decalin (**4b**), which is a typical kinetic product in the heterogeneous hydrogenation of **2** catalyzed by metal nanoparticles such as Ru and Rh.[27,28] Considering that the conventional high-pressure, high-temperature, long-time hydrogenation of arenes eventually yields the thermodynamically most stable *trans*-products under reversible hydrogenation–dehydrogenation equilibrium, our mechanochemical transfer hydrogenation at 100 °C for 10–60 min seems to be a mild and kinetically controlled reaction. In addition, we hypothesized that the further acceleration effect in our mechanochemical system can be derived from an increase in the frequency of contact between the catalyst and the substrate because of its highly concentrated conditions.

Then, we applied this methodology to an arene containing a bulky substituent, adamantane-annulated arene.[29] In 2024, we reported the synthesis of all-sp^3 carbon-containing diamondoids *via* hydrogenation of adamantane-annulated biphenyl (**5**).[10] We conducted catalytic hydrogenation of **5** with Rh–Pt/(DMPSi–Al_2O_3)[30,31] and $Sc(OTf)_3$ under 10 atom hydrogen gas at 125 °C for 72 h, affording two structural isomers of diamondoids, **6a** (as a thermodynamically favored product) and **6b** (as a kinetically favored product). Motivated by the harsh reaction conditions of the previous hydrogenation reaction and the higher catalytic activity of the proposed mechanochemical hydrogenation reaction, we examined the mechanochemical hydrogenation of **5**. As a result, fully and partially hydrogenated products **6b** and **6c** were obtained in 17 and 74% yields, respectively. The structure of the newly isolated **6c** was determined by X-ray crystallography (see ESI†). Notably, a difference in stereoselectivity was observed between the solution- and solid-state conditions. We assumed that the present mechanochemical hydrogenation preferentially afforded **6b** because the reaction proceeded in a shorter time at a lower temperature than that under solution-state conditions. Consequently, greater synthetic advantages in terms of faster reactions under milder conditions were observed in the present mechanochemical reaction.

We explored the substrate scope of various PAHs with a highly efficient and easy-to-handle mechanochemical hydrogenation (Fig. 3). The use of anthracene (**7a**), 9-anthraceneboronic acid bis(pinacol) ester (**7b**) and 9-anthracenecarboxylic acid (**7c**) resulted in the production of octahydroanthracene derivatives (**8a–8c**) in yields of 69%, 64% and 46%, respectively. In contrast, the reaction of methyl-9-anthracenecarboxylate (**7d**) afforded tetrahydroanthracene **8d** and dihydroanthracene **8d′** (see ESI†) as a mixture (40%, **8d**/**8d′** = 89 : 11). The use of 9-fluoroanthracene (**7e**) also afforded tetrahydroanthracene **8e** in 30% yield. The other polyaromatic compounds containing bromo, chloro, amino, formyl, hydroxy and ether groups, were found to be ineffective in this mechanochemical reaction in terms of low conversion of starting materials, poor functional group tolerability and formation of inseparable multiple isomers (see Fig. S2 in the ESI† for details). Then, we used π-extended acene such as tetracene (**7f**) and pentacene (**7g**) resulted in the formation of octahydrotetracene (**8f**) in 65% yield and hexadecahydropentacene (**8g**) as a single stereoisomer in 18% yield. Hydrogenation of 9,10-diphenylanthracene (**7h**) generated a separable mixture of terphenyl derivative **8h** (41%) and 1,4-diphenylnaphthalene derivative **8h′** (49%). In the reaction using 5,6,11,12-tetraphenyltetracene (rubrene, **7i**), both the sterically less hindered acene termini were hydrogenated to give 1,4,5,8-tetraphenylnaphthalene **8i** in 51% yield. In addition, a larger scale synthesis of **8i** was performed using a 10 mL stainless-steel jar and two stainless-steel balls (both with diameters of 10 mm) with 0.50 mmol (266.7 mg) **7i**, affording **8i** in a moderate yield of 36% (97.1 mg) after the reaction at same temperature for the same reaction time. The generation of the product in lower yield in the large-scale reaction can be attributed to the valence of the reaction scale, container surface area, and number of ball impacts; nevertheless, the yield and efficiency can be improved by further examination of the reaction parameters.[32] We then demonstrated the hydrogenation of larger PAHs, which typically show a low solubility and thus, a low reactivity for conventional hydrogenation. Using triphenylene (**7j**), dibenzo[*g*,*p*]chrysene (**7k**), and tribenzo[*b*,*e*,*k*]fluoranthene (**7l**) resulted in the formation of periphery-hydrogenated polyaromatic compounds **8j**, **8k**, and **8l** in 82%, 10%, and 53% yields, respectively. During the hydrogenation of **7k**, various partially hydrogenated products were formed, including **8k**, which made it difficult to isolate **8k** in high yield (see ESI† for details). The reactions with perylene (**7m**) and naphtho[8,1,2-*bcd*]perylene (**7n**)[15] also proceeded well to afford periphery-hydrogenated perylene derivatives **8m** (71%, 3 : 1 *cis*/*trans* mixture), **8m′** (12%), and **8n** (61%). The use of highly fused polyaromatic compounds such as coronene (**7o**), corannulene (**7p**), and dibenzo[*fg*,*ij*]-naphtho[1,2,3,4-*rst*]pentaphene (**7q**) afforded the periphery-hydrogenated PAHs **8o**, **8p**, and **8q** in 19%, 9%, and 11% yields, respectively. The reason for the low yields of these compounds is similar to that of **8k**: the formation of various partially hydrogenated products and isomers made separation difficult using silica gel column chromatography and size exclusion chromatography. Although the relative stereochemistry of **8p** could not be determined, it was obtained as a single stereoisomer. Single crystals of **8i** and **8o** were successfully obtained by recrystallization from $CHCl_3$/pentane, and their structures were elucidated by X-ray diffraction analysis. Unlike flat rubrene (5,6,11,12-tetraphenyltetracene),[33] **8i** possesses a highly twisted structure in the central naphthalene unit because of its congested peri-substituents and cyclohexane rings. Interestingly, only a few examples of synthesizing 1,4,5,8-tetraphenylnaphthalene are reported regardless of its simple structure.[34] In addition, highly twisted naphthalene structure with 26° of twisted angle (Φ) was observed, whose value is even larger than that of flat rubrene[33] ($\Phi = 0°$), considerable to those of π-extended rubrenes[35] ($\Phi = 20°$ in tetraphenylnaphthalene core), and smaller than that of octaphenyltetrabenzohexacene[36] (a twistacene) (average twisted angle of central tetracene core: $\Phi_{average} = 62°$) (see ESI† for details). In the crystallographic analysis of **8o**, the configuration of the four protons on the tertiary sp^3-carbons in **8o** was found to be *syn*-form, suggesting that the present multi-hydrogenation appears to be *cis*-

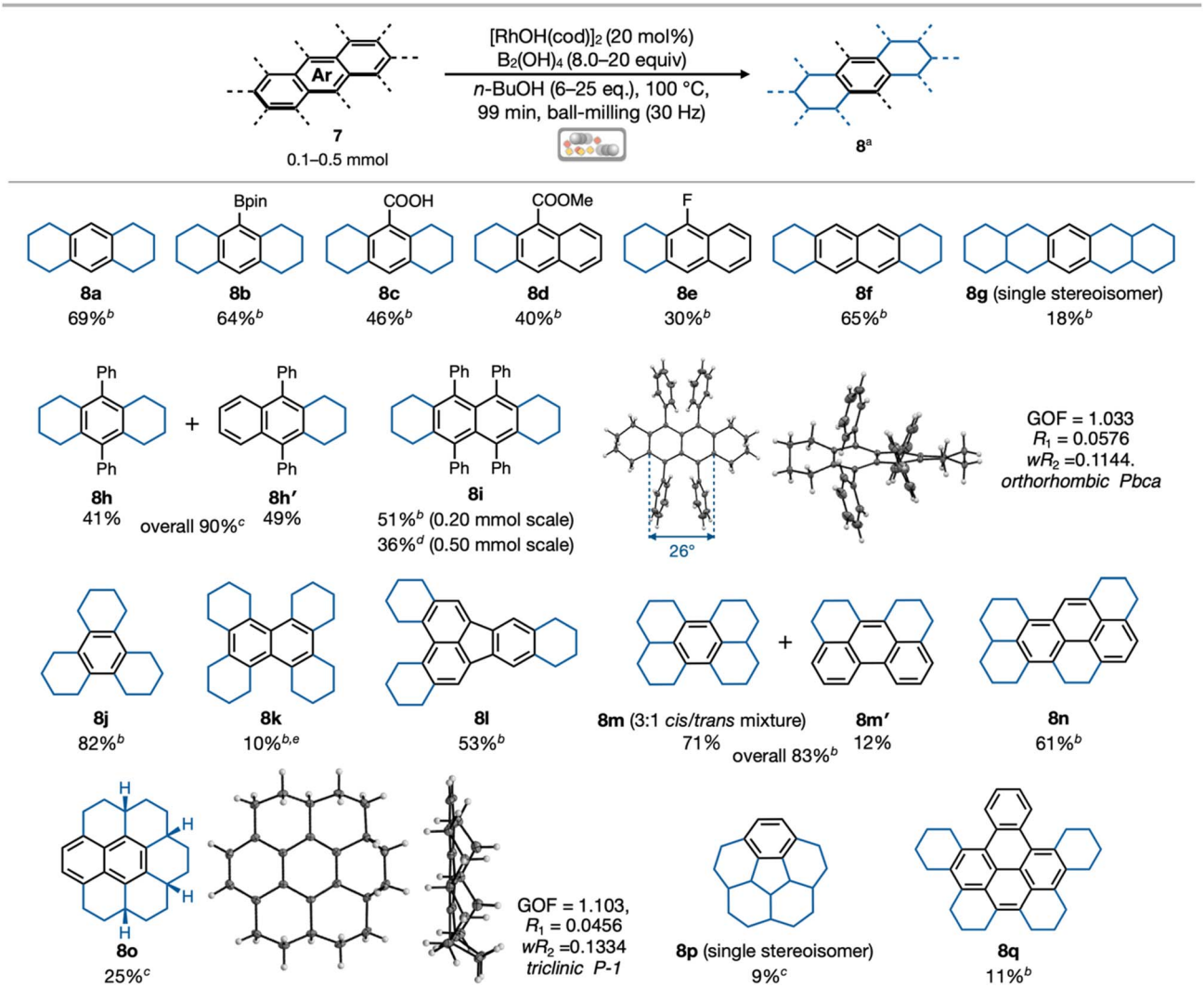

Fig. 3 Substrate scope in the mechanochemical transfer hydrogenation of PAHs and the ORTEP drawing of **8i**/**8o**. [a]Isolated yield. [b]Reactions were conducted in a 1.5 mL stainless-steel jar using a stainless-steel ball with a diameter of 7 mm. [c]Reactions were conducted in a 5.0 mL stainless-steel jar using a stainless-steel ball with a diameter of 10 mm. [d]Reactions were conducted in a 10 mL stainless-steel jar using two stainless-steel balls (both with a diameters of 10 mm) for 198 min. [e]Reaction time of ball milling was 60 min.

hydrogenation, as in a typical heterogeneous hydrogenation using metal nanoparticles such as Pd/C. This is in accordance with the mechanistic expectation of Dou.[14] that Rh nanoparticles are the active species in the catalytic system with $[RhOH(cod)]_2/B_2(OH)_4$/alcohol.

Because the obtained **8i** is a rare example of a 1,4,5,8-tetraphenylnaphthalene derivative and a lower homolog of rubrene and twistacene with a highly twisted structure, its electronic and photophysical properties are of interest. In the UV-vis absorption measurements of a solution of **8i** in THF ($c = 1.53 \times 10^{-5}$ M), two absorption maxima were observed at $\lambda_{abs} = 260$ and 322 nm; the absorption band was extended up to 400 nm (Fig. 4A). In addition, **8i** exhibited fluorescence upon excitation with 340 nm light, and broad emission band was observed along with an emission maximum at $\lambda_{em} = 407$. The absorption maxima were slightly red-shifted and emission maxima was slightly blue-shifted, compared with pristine 1,4,5,8-tetraphenylnaphthalene[32] ($\lambda_{abs} = 248$ and 334 nm, $\lambda_{em} = 437$ in cyclohexane). In the depiction of frontier molecular orbitals (MOs) calculated by the B3LYP/6-31G+(d,p) level of theory, HOMO and LUMO were mainly localized on naphthalene moiety, while the orbitals were slightly spread on phenyl rings and σ-bonds on benzylic C–H. In addition, terphenyl-like MO distributions appeared in other low-lying HOMO − 1 and HOMO − 2 and high-lying LUMO + 1 and LUMO + 2 (see ESI†). The photophysical properties of **8i** were further analyzed using time-dependent density functional theory (TD-DFT) calculations at the B3LYP/6-31+G(d,p) level of theory. The observed absorption maximum at $\lambda_{abs} = 322$ nm can be attributed to the allowed HOMO → LUMO transition ($\lambda = 352$ nm, oscillator strength (f) = 0.2104), whereas the second transition corresponding to HOMO → LUMO + 1 and HOMO − 1 → LUMO ($\lambda =$ 323 nm, $f = 0.0021$) and other transitions appear forbidden (see ESI† for other transitions).

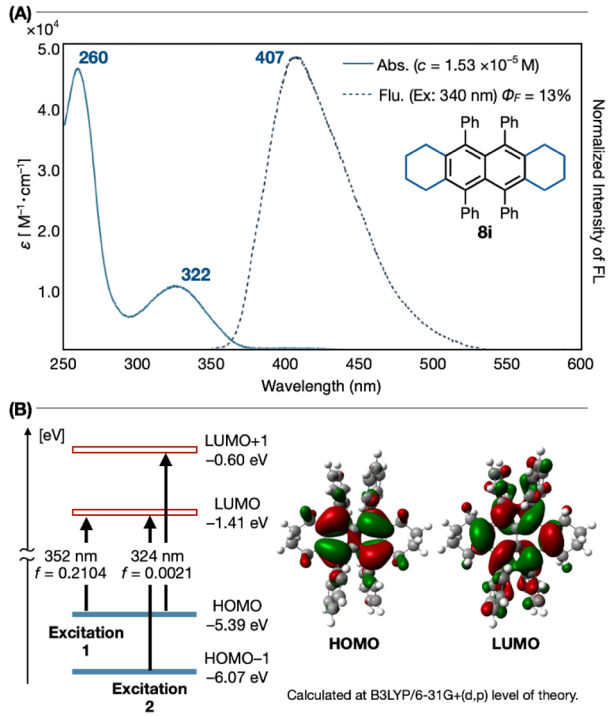

Fig. 4 (A) UV-vis absorption and emission spectra of **8i** ($c = 1.53 \times 10^{-5}$ M) in THF. Excitation light was 340 nm. (B) Possible transitions calculated by TD-DFT at the B3LYP/6-31G+(d,p) level of theory and depiction of frontier MOs.

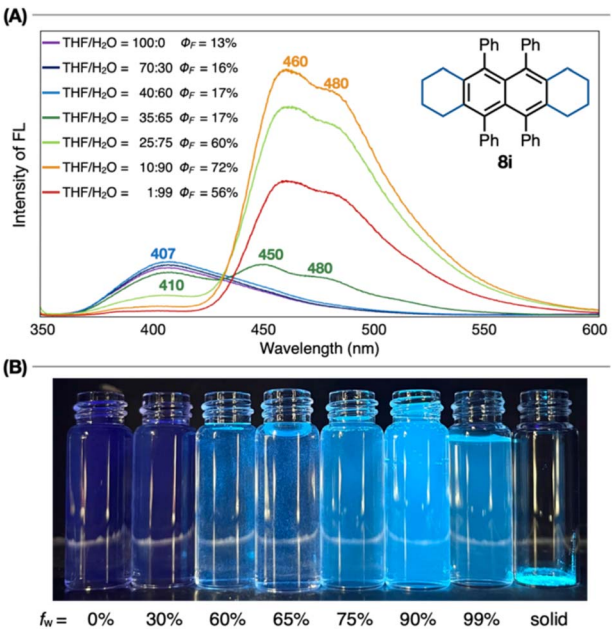

Fig. 5 (A) AIE emission of **8i** ($c = 1.93 \times 10^{-6}$ M) in THF/H_2O. Fluorescence spectra were recorded upon excitation at 340 nm. (B) Fluorescence photographs of solutions of **8i** in THF/water mixtures with different water contents. f_w is defined as fraction of water over total volumes of THF and H_2O.

Next, we investigated the solubility-derived properties of **8i**. This is typical of polyaromatic compounds, and planar PAHs generally show lower solubility in common organic solvents. A comparison of the solubilities of the mother- and periphery-hydrogenated aromatics is of interest. Indeed, rubrene shows low solubility (<0.2 mg mL^{-1}) in its saturated solution of hexane (see ESI†). Octahydrorubrene (**8i**) exhibited a higher solubility (0.6 mg mL^{-1} in hexane) than rubrene (see ESI†). Due to the slightly increased solubility and highly congested tetraphenyl moiety of **8i**, **8i** showed aggregation-induced emission (AIE)[37] in a THF/H_2O-mixed solvent system (Fig. 5) in the solutions of seven different ratios of THF/H_2O (100 : 0, 70 : 30, 40 : 60, 35 : 65, 25 : 75, 10 : 90, and 1 : 99). As illustrated in Fig. 5, the emission intensity at 407 nm gradually decreased as the THF/H_2O ratio shifted from 100 : 0 to 1 : 99, and new red-shifted emission peaks at 450 and 480 nm appeared at a ratio of 35 : 65. This is considered an AIE. The emission intensities became maximum values with enhanced fluorescent quantum yield ($\Phi_F = 72\%$) at the 10 : 90 ratio, whereas the intensities and Φ_F declined at the 1 : 99 possibly because the solvent composition became almost exclusively polar water solvents. While these AIE properties are similar to those of typical AIE molecules such as polyphenylarenes and tetraarylethenes,[37] the AIE properties of **8i** are unprecedented as 1,4,5,8-tetraphenylnaphthalene derivatives.

Conclusions

In summary, we developed a mechanochemical transfer hydrogenation of simple arenes and various PAHs as a novel synthetic method for periphery-hydrogenated PAHs. Using $[RhOH(cod)]_2$ as the catalyst and $B_2(OH)_4$/*n*-BuOH as the hydrogen donor under mechanochemical conditions, rapid and highly effective hydrogenation occurred, even under ambient pressure and atmosphere, affording sp^3-carbon-rich nanocarbons in a few hours. Furthermore, one of the hydrogenated products, the octahydrorubrene derivative (**8i**), exhibited characteristic photophysical properties such as AIE. We expect that the proposed mechanochemical hydrogenation method will contribute to the rapid and efficient synthesis of a novel class of sp^2/sp^3-carbon-conjugated hydrocarbons. Further studies on reactive species in the current catalytic system and application to larger nanographene is currently undergoing in our laboratory.

Data availability

Experimental and characterization data, including crystallographic data [**6c** (CCDC no. 2425787), **8i** (CCDC no. 2389852), and **8o** (CCDC no. 2389851)], photophysical measurements, and NMR spectra, as well as computational investigations. The data supporting this article have been included as part of the ESI.†

Author contributions

Y. T. synthesized, analyzed, and characterized all compounds and performed theoretical calculations with partial support from T. N., Y. M., and Y. O. Y. H. synthesized **6c** and elucidated its structure by X-ray crystallographic analysis. H. I. designed the project and target compounds, supervised the experiments, and conducted data analyses. H. I. and K. I. directed the project.

The draft manuscript was written by Y. T. and H. I., and all the authors finalized the manuscript through proofreading. All authors approved the final version of the manuscript.

Conflicts of interest

There are no conflicts to declare.

Acknowledgements

This study was supported by the Sumitomo Foundation (2300884 to H. I.), the Foundation of Public Interest of Tatematsu (22B025 to H. I.), the Kondo Memorial Foundation (2022-03, to H. I.), the NAGAI Foundation of Science and Technology (to H. I.), and JST-CREST (JPMJCR19R1 to A. Y.). Y. T. thanks the Interdisciplinary Frontier Next-Generation Researcher Program of the Tokai Higher Education and Research System for the fellowships. We thank Takato Mori and Daiki Imoto for their assistance with the X-ray crystallographic analyses. The computations were performed at the Research Center for Computational Science, Okazaki, Japan (Project No. 23-IMS-C061 and 24-IMS-C059).

Notes and references

1 (*a*) S. Allard, M. Forster, B. Souharce, H. Thiem and U. Scherf, *Angew. Chem., Int. Ed.*, 2008, **47**, 4070; (*b*) C. Wang, H. Dong, W. Hu, Y. Liu and D. Zhu, *Chem. Rev.*, 2012, **112**, 2208; (*c*) Y. Segawa, H. Ito and K. Itami, *Nat. Rev. Mater.*, 2016, **1**, 15002; (*d*) A. Narita, X. Wang, X. Fengb and K. Müllen, *Chem. Soc. Rev.*, 2015, **44**, 6616.

2 (*a*) R. M. Ferullo, C. E. Zubieta and P. G. Belelli, *Phys. Chem. Chem. Phys.*, 2019, **21**, 12012; (*b*) J. Son, S. Lee, S. J. Kim, B. C. Park, H. Lee, S. Kim, J. H. Kim, B. H. Hong and J. Hong, *Nat. Commun.*, 2016, **7**, 13261; (*c*) S. Cazaux, L. Boschman, N. Rougeau, G. Reitsma, R. Hoekstra, D. Teillet-Billy, S. Morisset, M. Spaans and T. Schlathölter, *Sci. Rep.*, 2016, **6**, 19835.

3 M. D. Watson, M. G. Debije, J. M. Warman and K. Müllen, *J. Am. Chem. Soc.*, 2004, **126**, 766.

4 X. Yao, X. Y. Wang, C. Simpson, G. M. Paternò, M. Guizzardi, M. Wagner, G. Cerullo, F. Scotognella, M. D. Watson, A. Narita and K. Müllen, *J. Am. Chem. Soc.*, 2019, **141**, 4230.

5 (*a*) M. Leccese, R. Jaganathan, L. Slumstrup, J. D. Thrower, L. Hornekær and R. Martinazzo, *Mon. Not. R. Astron. Soc.*, 2023, **519**, 5567; (*b*) H. Andrews, A. Candian and A. G. G. M. Tielens, *Astron. Astrophys.*, 2016, **595**, A23; (*c*) J. D. Thrower, E. E. Friis, A. L. Skov, B. Jørgensena and L. Hornekær, *Phys. Chem. Chem. Phys.*, 2014, **16**, 3381.

6 (*a*) R. H. Baker and R. D. Schuetz, *J. Am. Chem. Soc.*, 1947, **69**, 1250; (*b*) W. Kitching, H. A. Olszowy, G. M. Drew and W. Adcock, *J. Org. Chem.*, 1982, **47**, 5153; (*c*) R. J. Bonilla, B. R. James and P. G. Jessop, *Chem. Commun.*, 2000, 941; (*d*) B. Han, M. Zhang, H. Jiao, H. Ma, J. Wang and Y. Zhang, *RSC Adv.*, 2021, **11**, 39934; (*e*) A. A. Philippov, A. M. Chibiryaev and O. N. Martyanov, *Catal. Today*, 2021, **379**, 15.

7 (*a*) L. Rampazzo and A. Zeppa, *J. Electroanal. Chem.*, 1979, **105**, 221; (*b*) S. Friedman, S. Meltina, A. Svedi and I. Wender, *J. Org. Chem.*, 1959, **24**, 1287.

8 (*a*) P. P. Fu and R. G. Harvey, *Tetrahedron Lett.*, 1977, **5**, 415; (*b*) P. P. Fu, H. M. Lee and R. G. Harvey, *J. Org. Chem.*, 1980, **45**, 2797.

9 W. Lijinsky, G. Advani, L. Keefer, H. Y. Ramahi and L. Stach, *J. Chem. Eng. Data*, 1972, **17**, 100.

10 Y. Toyama, T. Yoshihara, H. Shudo, H. Ito, K. Itami and A. Yagi, *Chem. Lett.*, 2024, **53**, upad037.

11 (*a*) S. Origuchi, M. Kishimoto, M. Yoshizawa and S. Yoshimoto, *Angew. Chem., Int. Ed.*, 2018, **57**, 15481; (*b*) M. Müller, V. S. Iyer, C. Kübel, V. Enkelmann and K. Müllen, *Angew. Chem., Int. Ed. Engl.*, 1997, **36**, 1607.

12 G. Principi, F. Agresti, A. Maddalena and S. L. Russo, *Energy*, 2009, **34**, 2087.

13 C. Gelis, A. Heusler, Z. Nairoukh and F. Glorius, *Chem.–Eur. J.*, 2020, **26**, 14090.

14 Y. Wang, Z. Chang, Y. Hu, X. Lin and X. Dou, *Org. Lett.*, 2021, **23**, 1910.

15 (*a*) Y. Toyama, A. Yagi, K. Itami and H. Ito, *Chemrxiv*, 2024 Aug. 30th, preprint, DOI: **10.26434/chemrxiv-2024-ts4vf**; (*b*) K. Fujishiro, Y. Morinaka, Y. Ono, T. Tanaka, L. T. Scott, H. Ito and K. Itami, *J. Am. Chem. Soc.*, 2023, **145**, 8163.

16 (*a*) R. Takahashi, A. Hu, P. Gao, Y. Gao, Y. Pang, T. Seo, J. Jiang, S. Maeda, H. Takaya, K. Kubota and H. Ito, *Nat. Commun.*, 2021, **12**, 6691; (*b*) P. Gao, J. Jiang, S. Maeda, K. Kubota and H. Ito, *Angew. Chem., Int. Ed.*, 2022, **134**, e202207118; (*c*) R. Takahashi, P. Gao, K. Kubota and H. Ito, *Chem. Sci.*, 2023, **14**, 499; (*d*) K. Kubota, N. Shizukuishi, S. Kubo and H. Ito, *Chem. Lett.*, 2024, **53**, upae056; (*e*) K. Kubota, K. Kondo, T. Seo, M. Jin and H. Ito, *RSC Adv.*, 2023, **13**, 28652.

17 (*a*) S. L. James, C. J. Adams, C. Bolm, D. Braga, P. Collier, T. Friščić, F. Grepioni, K. D. M. Harris, G. Hyett, W. Jones, A. Krebs, J. Mack, L. Maini, A. G. Orpen, I. P. Parkin, W. C. Shearouse, J. W. Steedk and D. C. Waddelli, *Chem. Soc. Rev.*, 2012, **41**, 413; (*b*) G. W. Wang, *Chem. Soc. Rev.*, 2013, **42**, 7668; (*c*) J. L. Do and T. Friščić, *ACS Cent. Sci.*, 2017, **3**, 13; (*d*) K. Kubota and H. Ito, *Trends Chem.*, 2020, **2**, 1066.

18 (*a*) Y. Sawama, N. Yasukawa, K. Ban, R. Goto, M. Niikawa, Y. Monguchi, M. Itoh and H. Sajiki, *Org. Lett.*, 2018, **20**, 2892; (*b*) Y. Sawama, K. Ban, K. A. Suyama, H. Nakatam, M. Mori, T. Yamada, T. Kawajiri, N. Yasukawa, K. Park, Y. Monguchi, Y. Takagi, M. Yoshimura and H. Sajiki, *ACS Omega*, 2019, **4**, 11522.

19 (*a*) V. J. Kolcsár and G. Szőllősi, *ChemCatChem*, 2022, **14**, e202101501; (*b*) V. J. Kolcsár and G. Szőllősi, *Mol. Catal.*, 2022, **520**, 112162.

20 A. Y. Li, A. Segalla, C. J. Li and A. Moores, *ACS Sustainable Chem. Eng.*, 2017, **5**, 11752.

21 T. Portada, D. Margetić and V. Štrukil, *Molecules*, 2018, **23**, 3163.

22 M. Carta, A. L. Sanna, A. Porcheddu, S. Garroni and F. Delogu, *Sci. Rep.*, 2023, **13**, 2470.

23 B. G. Fiss, A. J. Richard and T. Friščić, *Can. J. Chem.*, 2021, **99**, 93.
24 (*a*) T. Seo, N. Toyoshima, K. Kubota and H. Ito, *J. Am. Chem. Soc.*, 2021, **143**, 6165; (*b*) Y. Gao, C. Feng, T. Seo, K. Kubota and H. Ito, *Chem. Sci.*, 2022, **13**, 430.
25 (*a*) B. L. Tran, J. L. Fulton, J. C. Linehan, J. A. Lercher and R. M. Bullock, *ACS Catal.*, 2018, **8**, 8441; (*b*) M. P. Wiesenfeldt, T. Knecht, C. Schlepphorst and F. Glorius, *Angew. Chem., Int. Ed.*, 2018, **57**, 8297.
26 (*a*) T. Seo, T. Ishiyama, K. Kubota and H. Ito, *Chem. Sci.*, 2019, **10**, 8202; (*b*) Z. J. Jiang, Z. H. Li, J. B. Yu and W. K. Su, *J. Org. Chem.*, 2016, **81**, 10049; (*c*) J. L. Howard, Y. Sagatov, L. Repusseau, C. Schotten and D. L. Browne, *Green Chem.*, 2017, **19**, 2798; (*d*) P. Ying, J. Yu and W. Su, *Adv. Synth. Catal.*, 2021, **363**, 1246.
27 E. Bresó-Femenia, B. Chaudret and S. Castillón, *Catal. Sci. Technol.*, 2015, **5**, 2741.
28 C. Hubert, E. G. Bilé, A. Denicourt-Nowicki and A. Roucoux, *Green Chem.*, 2011, **13**, 1766.
29 T. Yoshihara, H. Shudo, A. Yagi and K. Itami, *J. Am. Chem. Soc.*, 2023, **145**, 11754.
30 H. Miyamura, A. Suzuki, T. Yasukawa and S. Kobayashi, *J. Am. Chem. Soc.*, 2018, **140**, 11325.
31 H. Miyamura and S. Kobayashi, *Angew. Chem., Int. Ed.*, 2022, **61**, e202201203.
32 (*a*) G. Báti, S. Laxmi and M. C. Stuparu, *ChemSusChem*, 2023, **16**, e202301087; (*b*) D. M. Baier, T. Rensch, D. Dobreva, C. Spula, S. Fanenstich, M. Rappen, K. Bergheim, S. Grätz and L. Borchardt, *Chem.: Methods*, 2023, **3**, e202200058; (*c*) A. Stolle, R. Schmidta and K. Jacoba, *Faraday Discuss.*, 2014, **170**, 267.
33 O. D. Jurchescu, A. Meetsma and T. T. Palstra, *Acta Crystallogr.*, 2006, **B62**, 330.
34 E. D. Bergmann, S. Blumberg, P. Bracha and S. Epstein, *Tetrahedron*, 1964, **20**, 195.
35 W. Matsuoka, K. P. Kawahara, H. Ito, D. Sarlah and K. Itami, *J. Am. Chem. Soc.*, 2023, **145**, 658.
36 R. G. Clevenger, B. Kumar, E. M. Menuey and K. V. Kilway, *Chem.–Eur. J.*, 2018, **24**, 3113.
37 (*a*) Y. Hong, J. W. Y. Lam and B. Z. Tang, *Chem. Soc. Rev.*, 2011, **40**, 5361; (*b*) J. Mei, Y. Hong, J. W. Y. Lam, A. Qin, Y. Tang and B. Z. Tang, *Adv. Mater.*, 2014, **26**, 5429; (*c*) J. Mei, N. L. C. Leung, R. T. K. Kwok, J. W. Y. Lam and B. Z. Tang, *Chem. Rev.*, 2015, **115**, 11718; (*d*) X. Cai and B. Liu, *Angew. Chem., Int. Ed.*, 2020, **59**, 9868; (*e*) Z. Zhao H Zhang, J. W. Y. Lam and B. Z. Tang, *Angew. Chem., Int. Ed.*, 2020, **59**, 9888.